Electronic Supplementary Material (ESI) for Physical Chemistry Chemical Physics
This journal is © The Owner Societies 2014

Resolving Domain Structure for the Amorphous Iridium-oxide Water Oxidation Catalyst by X-ray Pair Distribution Function Analysis

Jier Huang,[a] James D. Blakemore,[b] Diego Fazi,[a] Oleksandr Kokhan,[a] Nathan D. Schley,[b] Robert H. Crabtree,[b]* Gary W. Brudvig,[b]* and David M. Tiede[a]*

[a] *Chemical Sciences and Engineering Division, Argonne National Laboratory, Argonne, Illinois 60439, United States.*
[b] *Department of Chemistry, Yale University, New Haven, Connecticut 06520, United States.*

E-mail:Robert.crabtree@yale.edu; gary.brudvig@yale.edu; tiede@anl.gov

Electrochemical Deposition of Iridium-oxide Amorphous Film. Starting materials and reagents were purchased from Sigma-Aldrich and used as received. The Ir precursor ($[Cp^*Ir(H_2O)_3]SO_4$) was prepared as previously described.[1,2] The amorphous iridium oxide film was electrodeposited onto 1-cm^2 ITO (indium tin oxide) electrode from a 1.5 mM Ir precursor with 0.1 M KNO_3 as electrolyte. The applied voltage is 1400 mV vs. NHE. After 2 hours of deposition, the blue layer film was air-dried and scraped off of the electrode surface. The sample was loaded as aqueous slurry into a 1 mm diameter Kapton tube.

High Energy X-ray Scattering (HEXS) Measurements and Pair Distribution Function (PDF) Analysis. High energy X-ray scattering (58 keV, λ= 0.2128 Å) measurement was carried out at beamline 11-ID-B of the Advanced Photon Source (APS) at Argonne National Laboratory. HEXS patterns were measured across the reciprocal space scattering range 0.5 $Å^{-1}$ to 24 $Å^{-1}$. The sample scattering patterns were corrected for solvent, container, and instrument background scattering, and then for multiple scattering, X-ray polarization, sample absorption, and Compton scattering using the program PDFgetX2[3] to yield the reduced scattering structure function *S(q)*, where $q=4\pi\sin(\Theta)/\lambda$ and 2Θ is the scattered angle. The direct Fourier transform of *S(q)* yielded the reduced pair distribution function, G(r):

$$G(r) = \frac{2}{\pi}\int_0^{q_{\max}} q[S(q)-1]\sin(qr)dq \qquad (1)$$

G(r) is termed the reduced PDF, defined by:

$$G(r) = 4\pi r[\rho(r) - \rho_0] \qquad (2)$$

where ρ(r) is the real space atomic pair electron density distribution function that is determined by atomic structure, and ρ_0 is the average electron density of the sample.

Model Calculations and Comparison to Experimental G(r) Pair Distribution Function. The approach for model calculation has been described in detail previously.[4] Briefly, G(r) was calculated from the various models originated from rutile structure of IrO_2 using equation 1. *S(q)* is calculated from:

$$S(q) = \frac{I^{coh}(q)}{\sum c_i f_i(q)^2} \qquad (3)$$

This journal is © The Owner Societies 2014

where $I^{coh}(q)$, the reduced total coherent scattering, was calculated from the Debye equation[5]:

$$I^{coh}(q) = \sum_{j}^{N}\sum_{k}^{N} A_j(q)A_k(q)\frac{(\sin qr_{jk})}{qr_{jk}}. \qquad (4)$$

In eqn. 4, $A_i(q)$ are the atomic scattering amplitudes derived from the atomic structure factors that were obtained by fitting atom scattering data in the international Tables for Crystallography[6] to a function, f_i, composed of five Gaussian components:[7,8]

$$A_j = f_j(q)e^{-b_j q^2/16\pi^2} - g_j(q). \qquad (5)$$

The atomic solvent excluded volume form factor, $g_j(q)$, was used to account for the scattering contribution due to solvent displacement and represented by a Gaussian form function.[9-11] Eqn. 5 also includes the atom-pair disorder factor, b_j, that is equivalent to the crystallographic Debye-Waller B-factor, $B = 8\pi^2\langle u^2\rangle$, where $\langle u^2\rangle$ is the average mean-squared atomic displacement, but written here in terms of the variable q rather than sin (Θ)/λ. In equation 4, the disorder factors are applied in the cases $j \neq i$ and set to zero when $j = i$. Thus, the S(q) calculations allow the effects of structural disorder to be accounted in two ways. For initial screening of G(r) calculated from model structures, the atom specific disorder factors were not used (b_i set to 0), and overall contributions of atomic disorder was included by using a q-dependent Gaussian dampening of S(q) as shown in data processing progression in figure S1 below. In addition, to test for the effects of additional, atom specific disorder, S(q) patterns were calculated using interactively adjusted non-zero b-factors for specific atoms, figure S2.

S(q) calculations based on a single explicit iridium oxide cluster do not account for the longer range amorphous structure or electron scattering contrast that occur in experimental small angle scattering for catalyst films. To account for these, scattering patterns calculated from models, $F(q) = q[S(q)-1]$, were modified, as illustrated in Figure S1a for model **4**, the 5 Ir-atom fragment originated from rutile structure of IrO_2 described in the text. The Fourier transforms of the original F(q) and modified mF(q) shown in Figure S1a yielded the G(r) shown in Figure S1b. G(r) calculated from other models were obtained using the same approach.

In Figure S3 an alternative approach was adopted to fit the experimental data. An automated algorithm was used which constructs a linear combination of G(r) functions obtained from four different iridium oxide clusters:

$$G_{tot}(r) = a_1 \cdot G_1(r) + a_2 \cdot G_2(r) + a_3 \cdot G_3(r) + a_4 \cdot G_4(r) \qquad (6)$$

and optimizes the multiplicative factors to obtain the best fit to the experimental G(r) using a *least squares* test for the N data sample points:

$$\chi^2 = C_{norm} \cdot \sum_{j=1}^{N} [G_{data}(r_j) - G_{tot}(r_j)]^2. \qquad (7)$$

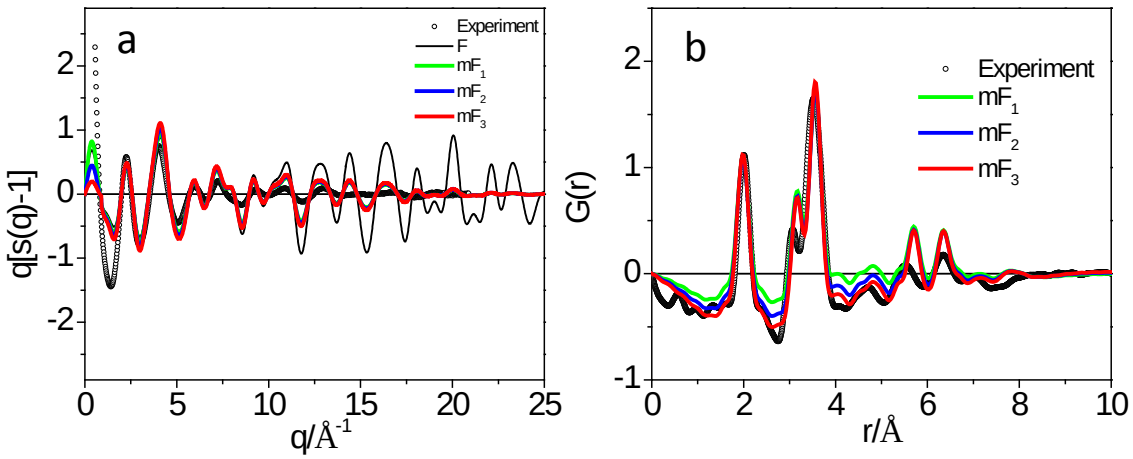

Figure S1. Part a. F(q) = q[S(q) - 1] calculated from the coordinates for model 4 using different amplitude processing protocols and comparison to the experimental F(q). F(q) was calculated directly from the coordinates. The modified F(q), mF_1, was obtained from F(q) by scaling with a q-dependent Gaussian amplitude dampening factor, $e^{-(\frac{q}{DW})^2}$, using DW = 12Å^{-1}. This scaling produces a q-dependent dampening of the interference pattern, and accounts for thermal and other sources for disorder that are present in the experimental sample but are absent in the fixed atomic coordinate model. The modified scattering patterns $mF_2(q)$ and $mF_3(q)$ were obtained from $mF_1(q)$ by adjusting the small angle scattering amplitude in the q-range below the zero crossing point at q=1.98 Å^{-1}. In $mF_2(q)$ and $mF_3(q)$ the amplitudes were scaled by factors of 0.5 and 0.2, respectively. This scaling has the effect of adjusting the X-ray scattering contrast. In the experimental sample, domain scattering is measured with respect to the electron density contrast provided by the film matrix, and has contributions from atomic packing in the distance range beyond 7 Å, and hence are absent from the domain models. Adjustments that decrease the small angle scattering amplitude have the effect of lowering the electron scattering contrast, which is the source of the negative "baselines" observed in the experimental G(r). Part b shows the G(r) calculated from the $mF_n(q)$ shown in Figure S1a.

This journal is © The Owner Societies 2014

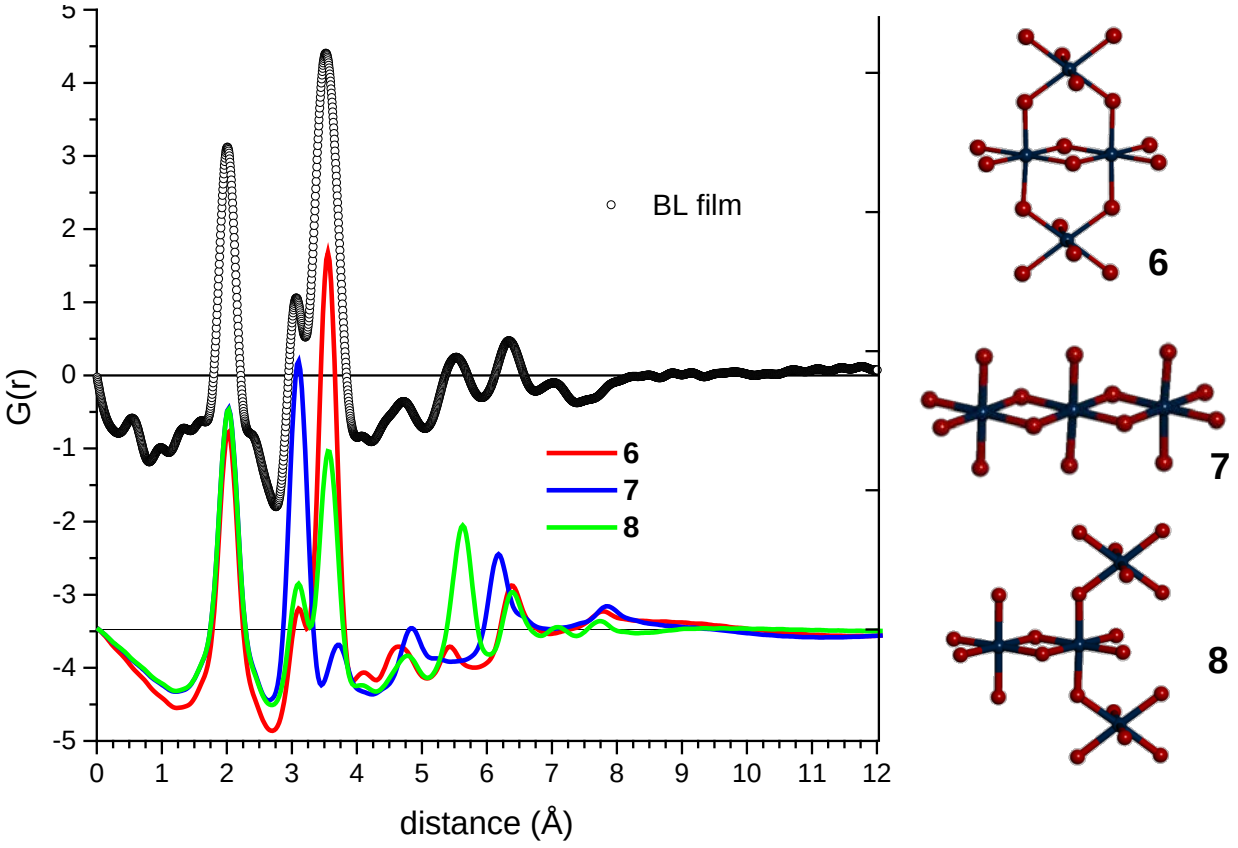

Figure S2. Comparison between the G(r) measured for the blue layer amorphous catalyst film, top, and the G(r) calculated for various atomic clusters extracted from the best fit, model **5** (described in the text). The substructures, 6, 7, 8, show correlations between specific atom pairs and the G(r), and how linear combinations of the substructures could be used to fit the experimental data.

This journal is © The Owner Societies 2014

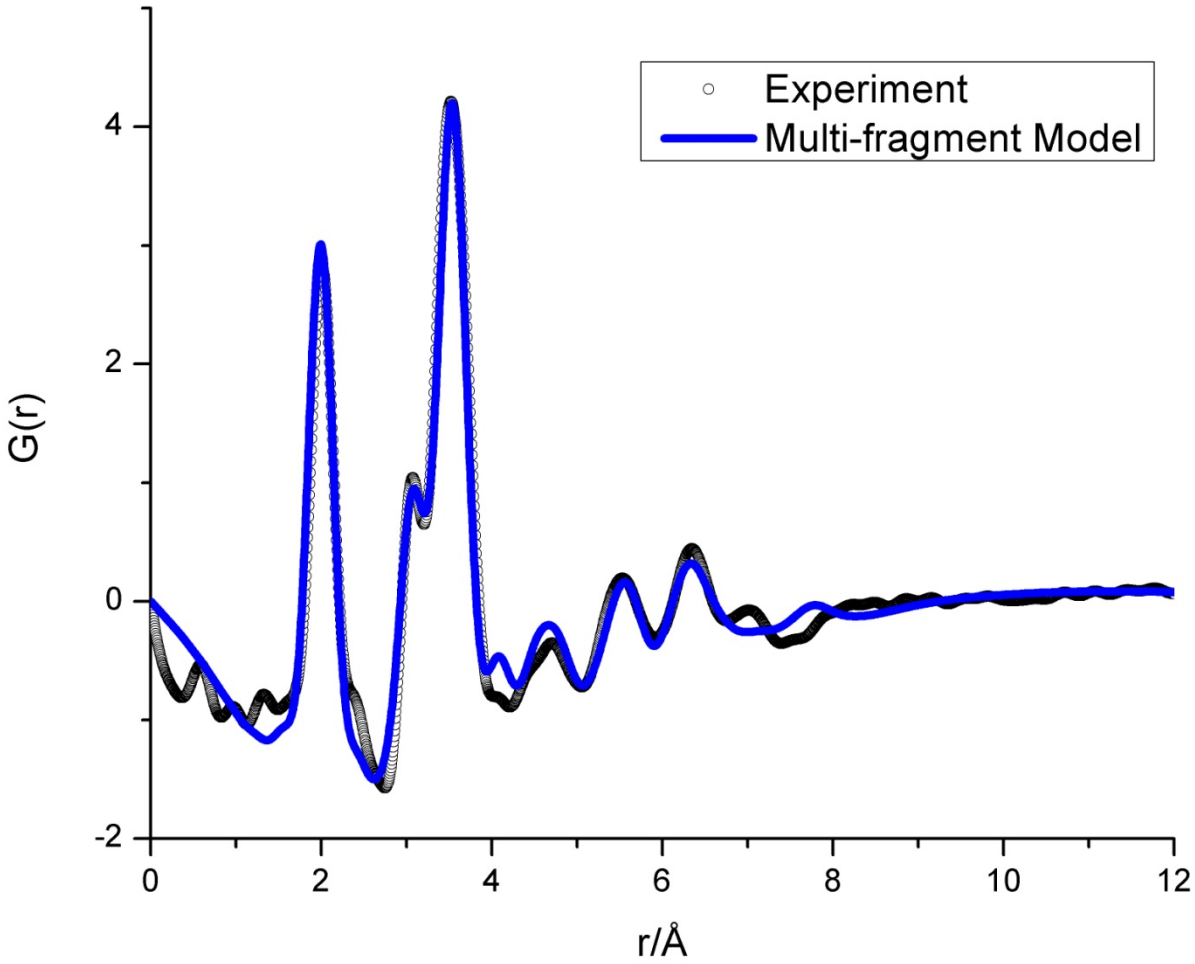

Figure S3. Comparison between the G(r) measured for the blue layer amorphous catalyst film (black circles) and the G(r) obtained from fitting the data as a distribution from library atomic clusters (blue line). The library of clusters consisted of model **5** described in the text, and the three substructures shown in Figure S2. The fit found the following population fractions:

Model 8: 0.500
Model 5: 0.413
Model 6: 0.087
Model 7: 0.000

This journal is © The Owner Societies 2014

Coordinates for Model 5

Ir4	4.514	4.516	6.228
Ir4	4.505	4.505	3.159
Ir4	4.512	4.498	0.089
Ir4	2.267	2.268	1.619
Ir4	6.752	6.752	1.586
O	5.924	5.927	6.228
O	3.103	3.106	6.228
O	3.648	5.382	7.807
O	5.380	3.650	7.807
O	3.595	5.415	4.698
O	5.414	3.596	4.697
O	5.907	5.907	3.171
O	3.103	3.103	3.216
O	5.413	3.596	1.628
O	3.604	5.406	1.619
O	3.646	5.364	-1.490
O	5.378	3.632	-1.490
O	5.914	5.900	0.009
O	1.400	1.401	0.040
O	1.400	1.401	3.199
O	0.856	3.678	1.619
O	3.678	0.857	1.619
O	3.110	3.096	0.021
O	5.329	8.156	1.586
O	8.174	5.347	1.586
O	7.618	7.618	0.007
O	7.618	7.618	3.166

References

(1) Blakemore, J. D.; Schley, N. D.; Olack, G. W.; Incarvito, C. D.; Brudvig, G. W.; Crabtree, R. H. *Chem Sci* **2011**, *2*, 94.
(2) Schley, N. D.; Blakemore, J. D.; Subbaiyan, N. K.; Incarvito, C. D.; D'Souza, F.; Crabtree, R. H.; Brudvig, G. W. *J Am Chem Soc* **2011**, *133*, 10473.
(3) Qiu, X.; Thompson, J. W.; Billinge, S. J. L. *J. Appl. Cryst.* **2004**, *37*, 678
(4) Du, P. W.; Kokhan, O.; Chapman, K. W.; Chupas, P. J.; Tiede, D. M. *J Am Chem Soc* **2012**, *134*, 11096.
(5) Warren, B. E. *X-Ray Diffraction*; Dover Publications, Inc: New York, 1990.
(6) Brown, P. J.; Fox, A. G.; Maslen, E. N.; O'Keeffe, M. A.; Willis, B. T. M. In *International Tables for Crystallography*; 2006 ed.; Prince, E., Ed.; John Wiley & Sons Ltd: 2006; Vol. C, p 554-595.
(7) Zhang, R.; Thiyagarajan, P.; Tiede, D. M., *J. Appl. Cryst.* **2000**, *33*, 565-568.
(8) Zuo, X.; Cui, G.; Mertz, K. M.; Zhang, L.; Lewis, F. D.; Tiede, D. M. , *Proc. Natl. Acad. Sci. U.S.A.* **2006**, *103*, 3534-3539.
(9) Fraser, R. D. B., MacRae, T. P. & Suzuki, E. (1978). *J. Appl. Cryst.* **11**, 693-694.
(10) Svergun, D., Barberato, C. & Koch, M. H. J. (1995). *J. Appl. Cryst.* **28**, 768-773.
(11) Zhang, R., Thiyagarajan, P. & Tiede, D. M. (2000). *J. Appl. Cryst.* **33**, 565-568.